Fumarylacetoacetate Hydrolase Knockout Rabbit Model for Hereditary Tyrosinemia Type 1

Li Li[1], Quanjun Zhang[1], Huaqiang Yang[1], Qingjian Zou[1], Chengdan Lai[1], Fei Jiang[1], Ping Zhao[1,2], Zhiwei Luo[1,2], Jiayin Yang[3], Qian Chen[4], Yan Wang[5,6], Philip N. Newsome[7,8], Jon Frampton[9], Patrick H. Maxwell[10], Wenjuan Li[1,2], Shuhan Chen[1,2], Dongye Wang[1,2], Tak-Shing Siu[11], Sidney Tam[11], Hung-Fat Tse[3,12,13], Baoming Qin[1], Xichen Bao[1,2], Miguel A. Esteban[1,2,12,*], and Liangxue Lai[1,*]

[1] CAS Key Laboratory of Regenerative Biology and Guangdong Provincial Key Laboratory of Stem Cells and Regenerative Medicine, Guangzhou Institutes of Biomedicine and Health, Chinese Academy of Sciences, Guangzhou 510530, China; [2] Laboratory of RNA, Chromatin, and Human Disease, Guangzhou Institutes of Biomedicine and Health, Chinese Academy of Sciences, Guangzhou 510530, China; [3] The Cardiology Division, Department of Medicine, Queen Mary Hospital, The University of Hong Kong, Hong Kong SAR, China; [4] Department of Ophthalmology, The Third Affiliated Hospital of Sun Yat-sen University, Guangzhou 510630, China; [5] State Key Laboratory of Organ Failure Research, Guangdong Provincial Key Laboratory of Viral Hepatitis Research, Guangdong Provincial Research Center for Liver Fibrosis, Department of Infectious Diseases and Hepatology Unit, Nanfang Hospital, Southern Medical University, Guangzhou 510515, China; [6] Biomedical Research Center, Southern Medical University, Guangzhou 510515, China; [7] Institute of Immunology and Immunotherapy, College of Medical and Dental Sciences, University of Birmingham, Birmingham B15 2TT, United Kingdom; [8] National Institute for Health Research (NIHR) Birmingham Liver Biomedical Research Unit and Centre for Liver Research, University of Birmingham, Birmingham B15 2TT, United Kingdom; [9] Institute of Cancer and Genomic Sciences, College of Medical and Dental Sciences, University of Birmingham, Birmingham B15 2TT, United Kingdom; [10] Cambridge Institute for Medical Research, Wellcome Trust/MRC Building, Cambridge CB2 0XY, United Kingdom; [11] Department of Clinical Biochemistry Unit, Queen Mary Hospital, Hong Kong; [12] Hong Kong-Guangdong Stem cell and Regenerative Medicine Research Centre, The University of Hong Kong and Guangzhou Institutes of Biomedicine and Health, China; [13] Shenzhen Institutes of Research and Innovation, The University of Hong Kong, Hong Kong SAR, China.

Running title: Fumarylacetoacetate hydrolase knockout rabbits

***To whom correspondence should be addressed:** Miguel A. Esteban (M.A.E) and Liangxue Lai (LX.L.), CAS Key Laboratory of Regenerative Biology and Guangdong Provincial Key Laboratory of Stem Cells and Regenerative Medicine, Guangzhou Institutes of Biomedicine and Health, Chinese Academy of Sciences, Guangzhou, China, Tel. 0086-20-32068110 (M.A.E) and 0086-20-2015346 (LX.L.), FAX: 0086-20-32015346 (M.A.E. and LX.L.), Email: miguel@gibh.ac.cn (M.A.E) and lai_liangxue@gibh.ac.cn (LX.L.)

Keywords: Hereditary tyrosinemia type 1, fumarylacetoacetate hydroxylase, transcription activator-like effector nucleases, genetically engineered rabbits, and liver regeneration

ABSTRACT

Hereditary tyrosinemia type 1 (HT1) is a severe human autosomal recessive disorder caused by the deficiency of fumarylacetoacetate hydroxylase (FAH), an enzyme catalyzing the last step in the tyrosine degradation pathway. Lack of FAH causes accumulation of toxic metabolites (fumarylacetoacetate and succinylacetone) in blood and tissues, ultimately resulting in severe liver and kidney damage with onset that ranges from infancy to adolescence. This tissue damage is lethal but can be controlled by administration of 2-(2-nitro-4-trifluoromethylbenzoyl)-1,3-cyclohex anedion (NTBC), which inhibits tyrosine catabolism upstream of the generation of fumarylacetoacetate and succinylacetone. Notably, in animals lacking *Fah*, transient withdrawal of NTBC can be used to induce liver damage and a concomitant regenerative response that stimulates the growth of healthy hepatocytes. Among other things, this model has raised tremendous interest for the *in vivo* expansion of human primary hepatocytes inside these animals, and for exploring experimental gene therapy and cell-based therapies. Here, we report the generation of *Fah* knockout rabbits via pronuclear-stage embryo microinjection of transcription activator-like effector nucleases (TALENs). *Fah*$^{-/-}$ rabbits exhibit phenotypic features of HT1 including liver and kidney abnormalities, but additionally develop frequent ocular manifestations likely caused by local accumulation of tyrosine upon NTBC administration. We also show that allogeneic transplantation of wild-type rabbit primary hepatocytes into *Fah*$^{-/-}$ rabbits enables highly efficient liver repopulation and prevents liver insufficiency and death. Due to significant advantages over rodents and their ease of breeding, maintenance, and manipulation compared to larger animals, including pigs, *Fah*$^{-/-}$ rabbits are an attractive alternative for modeling the consequences of HT1.

Animal models bearing mutations/truncations in genes causing human disease are essential to understand the mechanisms underlying those diseases, and to identify new diagnostic or therapeutic procedures. In some cases, the idiosyncrasy of human disease has also made these animals valuable for unexpected applications (1). One such example are *Fah*$^{-/-}$ mice (2), which have been genetically engineered to lack fumarylacetoacetate hydrolase (FAH), an enzyme responsible for catalyzing the last step in the degradation of the amino acid tyrosine (3). In humans, lack of FAH causes hereditary tyrosinemia type 1 (HT1), a rare autosomal recessive condition characterized by retrograde accumulation of toxic metabolites including fumarylacetoacetate and succinylacetone in blood and tissues, which ultimately causes liver failure and renal tubular dysfunction as the most prominent manifestations (4,5). Liver failure can develop acutely in the first few months after birth or be more progressive. Treatment of HT1 consists mainly of administration of 2-(2-nitro-4-trifluoromethylbenzoyl)-1,3-cyclohex anedion (NTBC), which inhibits the conversion of 4-hydroxyphenylpyruvate to homogentisic acid by 4-hydroxyphenylpyruvate dioxygenase, the second step in the tyrosine degradation pathway, thus preventing the accumulation of fumarylacetoacetate and succinylacetone (6). Yet, if patients are diagnosed too late or do not comply with NTBC treatment, there is end-stage liver disease with cirrhosis and high risk of hepatocellular carcinoma due to chronic damage. Notably, in *Fah*$^{-/-}$ mice, controlled withdrawal of NTBC can be used to cause liver damage in a desired manner, inducing the generation of a

regenerative response that allows repopulation of the damaged liver by the remaining normal hepatocytes after NTBC is added back (2,7). When *Fah*$^{-/-}$ mice are simultaneously deficient in key genes regulating the immune response (e.g., *Rag2* and/or *Il2rg*), the same principle allows liver repopulation with transplanted heterologous primary hepatocytes (8), stem cell-derived hepatocytes (9), or transdifferentiated hepatocytes (10,11) without immune rejection.

For a long time, genetic engineering of mammals has been mostly restricted to mice. This is because of the availability of mouse embryonic stem cells (ESCs) and the relative ease of manipulating these cells with traditional gene modification techniques. Genetically modified ESCs can then be injected into mouse blastocysts to produce chimeric animals with germ line transmission (12). Somatic cell modification and nuclear transfer has been traditionally an alternative for genetic engineering of species for which *bona fide* ESCs are not available, but the procedure is inefficient (13). More recently, the development of designer nuclease technologies (zinc-finger nucleases, transcription activator-like effector nucleases [TALENs], and clustered regularly interspaced short palindromic repeats [CRISPR]/CRISPR-associated protein 9 [Cas9] (14) has expanded significantly the repertoire of species (e.g., rats, rabbits, dogs, pigs, sheep, and cattle) (15-20) amenable to routine genetic engineering, and made the procedure a less time-consuming effort; *bona fide* rat ESCs were also isolated recently (21,22). Accordingly, several groups have reported the generation of *Fah*$^{-/-}$ pigs (23,24) and rats (25,26), which offer some advantages over *Fah*$^{-/-}$ mice.

Rabbits are widely used for animal experimentation. Their physiology is closer to humans than rodents, and they have relatively low cost maintenance and are easy to breed (27,28). Herein, we report the generation of *Fah*$^{-/-}$ rabbits by injecting TALENs into the cytoplasm of rabbit pronuclear-stage embryos. These *Fah*$^{-/-}$ rabbits have liver and kidney phenotypic features analogous to *Fah*$^{-/-}$ rodents and pigs, but also develop frequent ocular manifestations including corneal keratitis. We further show that allogeneic transplantation of wild-type rabbit primary hepatocytes achieves efficient liver repopulation and improves the liver function and survival rate of *Fah*$^{-/-}$ rabbits. These results demonstrate that genetically engineered *Fah*$^{-/-}$ rabbits are an attractive choice for modeling the consequences of HT1.

RESULTS

Construction of TALENs and generation of Fah knockout rabbits- We designed a pair of TALENs targeting exon 2 of the rabbit *Fah* gene (**Figure 1A**), and assembled them according to the Golden Gate method with the following codes: NI for adenine, NG for thymine, HD for cytosine, and NN for guanine. We injected different concentrations (10, 20, 30, 50, and 100 ng/μL) of *in vitro* transcribed TALEN-coding mRNAs into the cytoplasm of rabbit pronuclear-stage embryos (20,27), and then transferred the embryos into surrogate mothers. NTBC was administered to pregnant rabbits from day 15 of pregnancy to prevent intrauterine death (2). With the highest concentration of TALEN mRNAs, all foster mothers miscarried and no rabbits were born (**Table I**). The pregnancy was not affected with the other TALEN mRNA concentrations; a total of 31 rabbits were born and the ear tissue of each animal was collected for genotyping. With the lowest concentration of TALEN mRNAs, all 6 newborn rabbits were negative for gene targeting. Yet, we detected *Fah* mutations using 20 and 30 ng/μL, and the targeting efficiency was 100% (4 out of 4 newborns) using 50 ng/μL (**Table I**). These *Fah*

mutant rabbits were mostly mosaic, with different indels (insertions and/or deletions) within the *Fah* locus, as shown in (**Figure 1B)**. Through breeding of *Fah* mutant founder (F0) animals, we obtained a total of 9 *Fah*$^{-/-}$ first filial generation (F1) rabbits (**Figure 1C**) and 8 *Fah*$^{+/-}$ rabbits, which appeared healthy at birth. These animals were bred further to produce additional filial generations.

To ascertain the importance of NTBC administration in preventing death of *Fah*$^{-/-}$ rabbits, we prepared 13 *Fah*$^{-/-}$ rabbits and divided them into 3 groups, each with different NTBC administration modes (**Figure 1D**). The rabbits were closely monitored to collect blood before death and to store the tissues in good condition. In the first group, no NTBC was administered at any time after birth, and these animals died shortly (within 1 week after birth) (**Figure 1E**). In the second and third groups, NTBC was continuously administered until the rabbits were 2 weeks or 1 month old, respectively. Rabbits in the second group survived no longer than 3 weeks after birth, whilst rabbits in the third group were able to live as long as 4 months after birth (**Figure 1E**). Western blot analysis of liver tissue lysates from 2 dead *Fah*$^{-/-}$ rabbits showed that FAH was undetectable when compared with wild-type rabbits (**Figure 1F**). Likewise, heterozygous knockout (*Fah*$^{+/-}$) rabbits expressed half of the amount of protein of the wild-type. Thus, we have generated *Fah*$^{-/-}$ rabbits that can only be maintained alive with NTBC, and we next proceeded to study whether these animals develop characteristic phenotypic features of HT1.

Fah$^{-/-}$ *rabbits have liver and kidney phenotypic characteristics of HT1*- We dissected the bodies of dead *Fah*$^{-/-}$ rabbits belonging to the above-mentioned groups, and observed prominent liver swelling, hemorrhage, and yellow/green discoloration suggestive of both cholestasis and liver necrosis, in contrast to the normal aspect of their wild-type counterparts (**Figure 2A**). We also collected and sectioned the liver and kidney tissues for immunohistological analysis with FAH antibodies. As expected, FAH protein was completely absent in *Fah*$^{-/-}$ livers and kidneys, 2 tissues that normally express it at high level, but displayed strong staining in wild-type rabbits (**Figure 2B**). In addition, hematoxylin and eosin staining showed diffuse hepatocellular injury with dysplastic hepatocytes and tubule-interstitial nephritis in *Fah*$^{-/-}$ rabbits only (**Figure 2C**), both of which are hallmarks of HT1. Moreover, picrosirius red staining (29) revealed mild fibrosis in the liver of *Fah*$^{-/-}$ rabbits but not in wild-type (**Figure 2D**), which is in agreement with *Fah*$^{-/-}$ mice but contrasts with the development of cirrhosis in *Fah*$^{-/-}$ rats and pigs (25,30). In addition, we extracted serum from blood samples and analyzed the levels of alanine aminotransferase (ALT), aspartate aminotransferase (AST), and triglycerides, all of which are elevated as a consequence of liver damage (23). Significant increase of all 3 parameters was observed in *Fah*$^{-/-}$ rabbits maintained without NTBC compared to wild-type rabbits (**Figure 2E**). We also detected that tyrosine levels had increased in *Fah*$^{-/-}$ rabbits maintained without NTBC, illustrating that, as expected, deletion of *Fah* blocks the tyrosine metabolic pathway (2,5). Altogether, these results confirm that *Fah*$^{-/-}$ rabbits develop features similar to HT1 patients and rodent/pig models (5,7,23-26).

Ocular manifestations in Fah knockout rabbits- Ocular involvement is not frequent in HT1 patients but in those rare cases corneal keratitis is the main manifestation (31,32). This has been attributed to inflammation produced by local tyrosine deposition in the form of crystals, which is caused by low compliance with a low-protein diet and the secondary effect of using NTBC on tyrosine accumulation. Interestingly, in the course of our study, we noticed that *Fah*

knockout rabbits develop frequent ocular manifestations too. This problem was observed in all third filial generation *Fah*$^{-/-}$ rabbits and a small proportion of *Fah*$^{+/-}$ rabbits. Of note, although the latter were not treated with NTBC at any time after birth, it was administered to their mothers during pregnancy. We performed ophthalmological analysis of 2 *Fah*$^{+/-}$ rabbits compared to a wild-type rabbit. Through direct eye inspection, we discovered keratoleukoma accompanied by edema and opacity in both eyes of the 2 *Fah*$^{+/-}$ rabbits (**Figure 3A**). Using slit lamp imaging, we also noticed deeper chamber depth and lens opacification accompanied with dilated pupil and posterior synechia of the iris in the right eye of the first *Fah*$^{+/-}$ rabbit (**Figure 3B**), implying cataract and iritis. Moreover, in the same rabbit there was a pathogenic high intraocular pressure of 48.33 mm Hg in the left eye (**Figure 3C**), indicating secondary glaucoma, whilst intraocular pressure in the right eye was normal. Conversely, chamber depth and intraocular pressure were normal in the second *Fah*$^{+/-}$ rabbit (**Figure 3B and C**), and no significant cataract was found. In addition, hematoxylin and eosin staining showed edema and thickening in the corneal epithelium and stroma of both *Fah*$^{+/-}$ rabbits, and the corneal surface became irregular in particular in the left eye of the second *Fah*$^{+/-}$ rabbit (**Figure 3D**). Moreover, swelling, condensed nuclei, and fragmented bodies could be seen in corneal epithelial and stroma cells in both *Fah*$^{+/-}$ rabbits, indicating necrocytosis (**Figure 3D**). Therefore, there is frequent ocular involvement, mostly manifested as corneal keratitis, in *Fah* knockout rabbits.

Allogeneic primary hepatocyte transplantation rescues liver damage of Fah$^{-/-}$ *rabbits*- We then studied whether transplantation of *Fah*-competent hepatocytes could rescue the liver phenotype and prevent death of *Fah*$^{-/-}$ rabbits untreated with NTBC. First, to assess feasibility, we induced acute liver damage in wild-type rabbits with Concavalin A (33), which causes a rapid regenerative response that facilitates engraftment of transplanted cells, and 24 hours later 10^7 rabbit primary hepatocytes extracted from a healthy wild-type rabbit were injected intrasplenically. To assist with their identification, transplanted hepatocytes were labeled with DiI, as this fluorescent compound can last as long as 1 month *in vivo* (34,35). The recipient animals were immunosuppressed with Cyclosporin A starting 24 hours before transplantation. We observed a large number of DiI-positive cells in liver sections 3 weeks after transplantation, proving the efficacy of the approach (**Figure 4A**). Next, we transplanted wild-type rabbit primary hepatocytes into 2 *Fah*$^{-/-}$ rabbits that had been treated with NTBC after birth. A wild-type rabbit and a non-transplanted *Fah*$^{-/-}$ rabbit treated with NTBC were used as controls. NTBC was gradually decreased in the 3 *Fah*$^{-/-}$ rabbits, and completely withdrawn 1 week after the transplantation (**Figure 4B**). One month after NTBC withdrawal, a small liver biopsy was obtained from one of the transplanted *Fah*$^{-/-}$ rabbits and the non-transplanted *Fah*$^{-/-}$ rabbit for histological analysis. Approximately 30% of liver cells in the examined liver sections of the transplanted *Fah*$^{-/-}$ rabbit were DiI-positive at this time point (**Figure 4C**). Likewise, FAH immunohistochemistry confirmed significant engraftment of FAH-positive hepatocytes in the same *Fah*$^{-/-}$ transplanted rabbit, and these hepatocytes displayed normal morphology in contrast with damaged cells in non-engrafted areas (**Figure 5A**). We also measured weight in these *Fah*$^{-/-}$ rabbits and the wild-type control over the post-transplantation period. We noticed that, 11 weeks after NTBC withdrawal the *Fah*$^{-/-}$ rabbit that did not receive transplantation showed a 40% decrease in body weight and died shortly after, whilst the wild-type and *Fah*$^{-/-}$ rabbits receiving

allogeneic hepatocyte transplantation had similar weight and appeared healthy (**Figure 5B and C**). In addition, we performed serum biochemical analysis over the post-transplantation period to see whether liver function can be recovered in *Fah*$^{-/-}$ rabbits compared to the control. Indeed, ALT and AST values of wild-type and a transplanted *Fah*$^{-/-}$ rabbit were alike at week 10 post-transplantation, whilst the non-transplanted *Fah*$^{-/-}$ rabbit showed significantly higher values (**Figure 5D and E**). Interestingly, we also observed more engrafted FAH-positive cells at three months in the transplanted *Fah*$^{-/-}$ rabbits (**Figure 5F and G**), indicating long-term stability of the engrafted cells and suggesting *in vivo* proliferation. These data prove the utility of *Fah*$^{-/-}$ rabbits as tools for testing experimental methodologies involving liver cell transplantation.

DISCUSSION

Patients with HT1 are treated with NTBC and dietary restrictions but this is not curative and, besides, a number of individuals fail to respond and require liver transplantation (7). Because shortage of donors limits organ transplantation, other therapeutic strategies (e.g., stem cell-based or gene therapy approaches) are urgently needed to treat this patient population. Appropriate preclinical animal models are required for testing these experimental therapies and although *Fah*$^{-/-}$ mice present many phenotypic features of HT1, their physiology (e.g., inflammatory responses (36)) differs significantly from humans. Likewise, their small size and short life span pose a limitation for analytical studies and long-term assessments. Aiming to solve these issues, *Fah*$^{-/-}$ rats (25,26), and in particular pigs (23,24), have been generated recently. However, whilst pigs have many advantages over rodents for HT1 disease modeling, their handling and breeding is laborious and costly.

Rabbits are excellent animals for state-of-the-art animal experimentation. They are closer phylogenetically to primates than rodents and have a longer life span (8-10 years), whilst their medium size, short pregnancy period (1 month versus 4 in pigs), and relatively straightforward husbandry requirements facilitate production of large cohorts at relatively low cost (27,28). Like pigs, rabbits also have a more diverse genetic background than rodents, a situation that is closer to that in humans. Notably, the first transgenic rabbits were generated over 3 decades ago (37,38), but the lack of *bona fide* rabbit ESCs for more complex genetic engineering and the inefficiency of rabbit somatic cell nuclear transfer (39) hampered the development of the field until the arrival of highly efficient designer nuclease technologies (20,40-42).

Our work presented here is the first description of genetically engineered *Fah*$^{-/-}$ rabbits. We used TALEN mRNA microinjection into pronuclear-stage rabbit embryos (20) rather than the CRISPR/Cas9 system (40,43) because we envisaged that for embryo injections the toxicity and off-target effects of the former are easier to control (44), though recent improvements of the CRISPR/Cas9 technique could solve this issue (45). *Fah*$^{-/-}$ rabbits display liver and kidney manifestations of the human genetic disorder but also have frequent ocular alterations (mostly corneal keratitis). Ocular involvement is rare in patients with HT1 but frequent in patients with tyrosinemia type II (46), which is produced by mutations in tyrosine transaminase, the enzyme undertaking the first step of tyrosine catabolism. As with tyrosinemia type II, corneal keratitis in HT1 patients, and possibly *Fah* knockout rabbits too, is caused by enhanced local accumulation of tyrosine, which is boosted by NTBC (31,32). The frequency with which ocular manifestations happen in *Fah*$^{-/-}$ rabbits potentially makes them a

useful model for studying how to prevent and treat this potential complication in HT1 patients. *Fah*$^{-/-}$ rabbits did not develop cirrhosis in our study, although it is likely that varying the NTBC administration/withdrawal routine and allowing more chronic damage would induce it. Besides being an excellent choice for modeling HT1 and studying chronic liver damage, *Fah*$^{-/-}$ rabbits could also be employed for testing gene therapy approaches, which have proved successful in *Fah*$^{-/-}$ mice and pigs but require additional studies to evaluate long-term safety and efficacy (24). In addition, *Fah*$^{-/-}$ rabbits could be exceptional bioreactors for growing primary human hepatocytes for *in vivo* human disease modeling (e.g., hepatitis B or C), potential xenotransplantation, or for *in vitro* studies, but this would require producing *Fah*$^{-/-}$*Rag2*$^{-/-}$*Il2rg*$^{-/-}$ rabbits to avoid immune rejection. Such triple knockout animals would be valuable too as preclinical models for experimental stem cell based-therapies, including the transplantation of hepatocyte-like cells derived from induced pluripotent stem cells (11) or produced through transdifferentiation (10,11). Given the time and cost of pursuing this approach in pigs, rabbits offer an attractive option.

In summary, we have demonstrated that *Fah*$^{-/-}$ rabbits are a promising alternative for modeling HT1 and for developing therapeutic strategies aiming to cure this disease. From a wider perspective, our work also shows that genetically engineered rabbits offer a powerful approach to recapitulating human disease.

EXPERIMENTAL PROCEDURES

Animals and ethics statement- New Zealand white rabbits were obtained from the Laboratory Animal Centre of Southern Medical University (Guangzhou, China). All rabbit experiments were conducted under the approval of the Animal Care and Use committee of the Guangzhou Institutes of Biomedicine and Health (ID 2012040) and the Department of Science and Technology of Guangdong Province (ID SYXK 2005-0063). Animals were observed at least once daily for clinical signs and symptoms consistent with acute liver failure. To obtain *Fah*$^{-/-}$ and *Fah*$^{+/-}$ F1 rabbits, we breed F0 animals with each other, and then we bred F0 with F1 and F1 with F1, and so on, for producing other filial generations. For details of which rabbits were used in each experiment and their respective genotypes see **Supplemental Table I**. Pregnant rabbits giving birth to *Fah*$^{-/-}$ rabbits received NTBC 7.5 mg/L per 200 mL of drinking water per day beginning on day 15 of pregnancy. The same dose was used for maintenance of *Fah*$^{-/-}$ rabbits. Ophtalmological evaluation was performed in Zhongshan Ophthalmic Center, Sun Yat-sen University.

TALEN preparation, embryo microinjection, and embryo transfer- TALENs were designed and assembled according to the Golden Gate assembly method (27). *In vitro* transcribed TALEN mRNAs were prepared using mMESSAGE mMACHINE® T7 Kit (Ambion, Austin, TX, USA) and purified using RNeasy Mini Elute Cleanup Kit (Qiagen, Valencia, CA, USA). The TALEN microinjection procedure was essentially as described previously (27). Briefly: 6-8 months old female rabbits were induced to superovulate with 50 IU FSH every 3 hours for 3 days, mated with male rabbits about 72 hours later, and injected with 100 IU of human chorionic gonadotropin. Female rabbits were euthanized 18 hours after injection and the oviducts were flushed with pre-warmed embryo manipulation medium for collecting embryos at the pronuclear stage. Mixed *in vitro* transcribed TALEN mRNAs were microinjected into the cytoplasm, and then embryos were transferred to EBSS medium for *in vitro* culture in a 5% CO2 incubator at 38.5°C with 100% humidity.

Approximately 15-30 good quality (as judged by microscope inspection) injected embryos were transferred into unilateral pavilions of the oviducts for each recipient mother.

Genotyping- DNA of newborn rabbits was extracted from a small piece of ear tissue using a Hipure Tissue DNA Mini Kit (Magen, Beijing, China) following the manufacturer's protocol. PCR products spanning the TALEN target sites were amplified with KOD-Plus-Neo DNA Polymerase (TOYOBO, Tokyo, Japan) with the following primers: 5'-GCACTTGAGCCATCGTCCGT (FAH-F) and 5'-ACCAGCAGCAGGCAATCCCA (FAH-R), and then sequenced.

Western blot assay- For Western blotting, liver tissue samples were homogenized in RIPA buffer and centrifuged at 14,500 g at 4˚C for 30 minutes; supernatants were then collected and protein concentration quantified. Lysates were subjected to 10% polyacrylamide-SDS gel electrophoresis, followed by immunoblotting onto a polyvinylidene fluoride membrane (Millipore, Temecula, CA, USA). Membranes were blocked with 5% evaporated milk in TBST for 2 hours and incubated overnight at room temperature with primary antibodies against FAH (ab140167, Abcam, Cambridge, UK). Membranes were then incubated with a secondary HRP-conjugated anti-rabbit antibody (sc-2004, Santa Cruz, CA, USA) for 60 minutes at room temperature and imaged using a SuperSignal™ West Pico Chemiluminescence Substrate kit (Thermo, Rockford, USA). ACTIN antibody (sc-47778, Santa Cruz, CA, USA) was probed as loading control.

Histology- Liver and kidney tissues were fixed with 4% neutral buffered paraformaldehyde for 48 hours and processed for paraffin embedding and sectioning. For immunohistochemistry staining, antigen retrieval was performed in a 1 M citrate buffer (pH 6.0) bath for 20 minutes. Tissues were immunostained with anti-FAH primary antibodies (ab140167) and visualized using VECTASTAIN Elite ABC HRP Kit (Vector Laboratories, CA, USA). Hematoxylin and eosin staining and picrosirius red staining were prepared using standard protocols.

Serum analysis- Blood was obtained via puncture of the ear vein using heparinized tubes. Serum was separated by centrifugation at 900 g for 20 minutes and stored at -80˚C prior to biochemistry and amino acid analysis. Concentration of ALT, AST, and triglycerides was measured with a CL-8000 Hitachi 7180 automatic biochemical analyzer (Shimadzu, Kyoto, Japan). Tyrosine was quantified by liquid chromatography mass spectrometry using the ABI 3200 Q TRAP LC–MS/MS system (Applied Biosystems, Foster City, CA, USA).

Allogeneic hepatocyte transplantation- Fresh hepatocytes were isolated from wild-type rabbit livers by in situ collagenase perfusion as previously reported (47). Briefly, the liver was perfused with calcium- and magnesium-free Hank's Balanced salt solution (Thermo, Rockford, USA) supplemented with 0.5 mM EGTA for 10 minutes and 10 mM HEPES for 3 minutes. The solution was changed to EBSS supplemented with 0.1 mg/ml collagenase IV (Sigma, St Louis, MO, USA) for 10 minutes. The liver was then gently minced in the second solution and filtered through 150 µm, 75 µm, 50 µm, and 37.5 µm nylon mesh, sequentially. After centrifugation at 50 g for 5 minutes, the pellet was washed with 4.5 g/mL DMEM 3 times at 50 g for 2 minutes. The number and viability of cells was assessed by trypan blue. 10^7 viable cells were then incubated in a 20 µM DiI solution (Sigma, St Louis, MO, USA) for 5 minutes at 37˚C and for 15 minutes at 4˚C for labeling, and washed in 4.5 g/mL DMEM. Eventually, 10^7 hepatocytes in 2.5 mL Clonetics®

Hepatocyte culture medium (Lonza, Walkersville, MD, USA) were injected into the spleen of recipient rabbits via a small flank incision. Concavalin A and Cyclosporin A were purchased from Sigma.

Acknowledgments: We would like to thank the members in Laboratory Animal Center of the Guangzhou Institutes of Biomedicine and Health for histological analysis, and also Yan Chen for technical advice.

Conflict of interest: none.

Author contributions: M.A.E. and LX.L. had the idea; L.L., LX.L., and M.A.E. designed the experiments; L.L. and M.A.E. analyzed the data; L.L. conducted most of the experiments; all other authors contributed to the experiments or provided critical advice; M.A.E. and LX.L. provided funding; M.A.E. and L.L. wrote the manuscript, and M.A.E. and LX.L. approved the final version for submission.

REFERENCES

1. Nakamura, K., Tanaka, Y., Mitsubuchi, H., and Endo, F. (2007) Animal models of tyrosinemia. *J Nutr* **137**, 1556-1560
2. Grompe, M., Lindstedt, S., al-Dhalimy, M., Kennaway, N. G., Papaconstantinou, J., Torres-Ramos, C. A., Ou, C. N., and Finegold, M. (1995) Pharmacological correction of neonatal lethal hepatic dysfunction in a murine model of hereditary tyrosinaemia type I. *Nat Genet* **10**, 453-460
3. Grompe, M. (2001) The pathophysiology and treatment of hereditary tyrosinemia type 1. *Semin Liver Dis* **21**, 563-571
4. Russo, P., and O'Regan, S. (1990) Visceral pathology of hereditary tyrosinemia type I. *Am J Hum Genet* **47**, 317-324
5. Vogel, A., van Den Berg, I. E., Al-Dhalimy, M., Groopman, J., Ou, C. N., Ryabinina, O., Iordanov, M. S., Finegold, M., and Grompe, M. (2004) Chronic liver disease in murine hereditary tyrosinemia type 1 induces resistance to cell death. *Hepatology* **39**, 433-443
6. Lindstedt, S., Holme, E., Lock, E. A., Hjalmarson, O., and Strandvik, B. (1992) Treatment of Hereditary Tyrosinemia Type-I by Inhibition of 4-Hydroxyphenylpyruvate Dioxygenase. *Lancet* **340**, 813-817
7. Ashorn, M., Pitkanen, S., Salo, M. K., and Heikinheimo, M. (2006) Current strategies for the treatment of hereditary tyrosinemia type I. *Paediatric drugs* **8**, 47-54
8. Azuma, H., Paulk, N., Ranade, A., Dorrell, C., Al-Dhalimy, M., Ellis, E., Strom, S., Kay, M. A., Finegold, M., and Grompe, M. (2007) Robust expansion of human hepatocytes in Fah(-/-)/Rag2(-/-)/Il2rg(-/-) mice. *Nat Biotechnol* **25**, 903-910
9. Huch, M., Dorrell, C., Boj, S. F., van Es, J. H., Li, V. S., van de Wetering, M., Sato, T., Hamer, K., Sasaki, N., Finegold, M. J., Haft, A., Vries, R. G., Grompe, M., and Clevers, H. (2013) In vitro expansion of single Lgr5+ liver stem cells induced by Wnt-driven regeneration. *Nature* **494**, 247-250
10. Huang, P., He, Z., Ji, S., Sun, H., Xiang, D., Liu, C., Hu, Y., Wang, X., and Hui, L. (2011) Induction of functional hepatocyte-like cells from mouse fibroblasts by defined factors. *Nature* **475**, 386-389
11. Zhu, S., Rezvani, M., Harbell, J., Mattis, A. N., Wolfe, A. R., Benet, L. Z., Willenbring, H., and Ding, S. (2014) Mouse liver repopulation with hepatocytes generated from human fibroblasts. *Nature* **508**, 93-97
12. Capecchi, M. R. (1989) Altering the genome by homologous recombination. *Science* **244**, 1288-1292
13. Lai, L., Kolber-Simonds, D., Park, K. W., Cheong, H. T., Greenstein, J. L., Im, G. S., Samuel, M., Bonk, A., Rieke, A., Day, B. N., Murphy, C. N., Carter, D. B., Hawley, R. J., and Prather, R. S. (2002) Production of alpha-1,3-galactosyltransferase knockout pigs by nuclear transfer cloning. *Science* **295**, 1089-1092
14. Gaj, T., Gersbach, C. A., and Barbas, C. F., 3rd. (2013) ZFN, TALEN, and CRISPR/Cas-based methods for genome engineering. *Trends Biotechnol* **31**, 397-405
15. Carlson, D. F., Lancto, C. A., Zang, B., Kim, E. S., Walton, M., Oldeschulte, D., Seabury, C.,

Sonstegard, T. S., and Fahrenkrug, S. C. (2016) Production of hornless dairy cattle from genome-edited cell lines. *Nat Biotechnol* **34**, 479-481

16. Zou, Q., Wang, X., Liu, Y., Ouyang, Z., Long, H., Wei, S., Xin, J., Zhao, B., Lai, S., Shen, J., Ni, Q., Yang, H., Zhong, H., Li, L., Hu, M., Zhang, Q., Zhou, Z., He, J., Yan, Q., Fan, N., Zhao, Y., Liu, Z., Guo, L., Huang, J., Zhang, G., Ying, J., Lai, L., and Gao, X. (2015) Generation of gene-target dogs using CRISPR/Cas9 system. *J Mol Cell Biol* **7,** 580-583
17. Yang, D., Yang, H., Li, W., Zhao, B., Ouyang, Z., Liu, Z., Zhao, Y., Fan, N., Song, J., Tian, J., Li, F., Zhang, J., Chang, L., Pei, D., Chen, Y. E., and Lai, L. (2011) Generation of PPARgamma mono-allelic knockout pigs via zinc-finger nucleases and nuclear transfer cloning. *Cell Res* **21**, 979-982
18. Geurts, A. M., Cost, G. J., Freyvert, Y., Zeitler, B., Miller, J. C., Choi, V. M., Jenkins, S. S., Wood, A., Cui, X., Meng, X., Vincent, A., Lam, S., Michalkiewicz, M., Schilling, R., Foeckler, J., Kalloway, S., Weiler, H., Menoret, S., Anegon, I., Davis, G. D., Zhang, L., Rebar, E. J., Gregory, P. D., Urnov, F. D., Jacob, H. J., and Buelow, R. (2009) Knockout rats via embryo microinjection of zinc-finger nucleases. *Science* **325**, 433
19. Wu, M., Wei, C., Lian, Z., Liu, R., Zhu, C., Wang, H., Cao, J., Shen, Y., Zhao, F., Zhang, L., Mu, Z., Wang, Y., Wang, X., Du, L., and Wang, C. (2016) Rosa26-targeted sheep gene knock-in via CRISPR-Cas9 system. *Sci Rep* **6**, 24360
20. Song, J., Zhong, J., Guo, X., Chen, Y., Zou, Q., Huang, J., Li, X., Zhang, Q., Jiang, Z., Tang, C., Yang, H., Liu, T., Li, P., Pei, D., and Lai, L. (2013) Generation of RAG 1- and 2-deficient rabbits by embryo microinjection of TALENs. *Cell Res* **23**, 1059-1062
21. Buehr, M., Meek, S., Blair, K., Yang, J., Ure, J., Silva, J., Mclay, R., Hall, J., Ying, Q. L., and Smith, A. (2008) Capture of Authentic Embryonic Stem Cells from Rat Blastocysts. *Cell* **135**, 1287-1298
22. Li, P., Tong, C., Mehrian-Shai, R., Jia, L., Wu, N., Yan, Y., Maxson, R. E., Schulze, E. N., Song, H., Hsieh, C. L., Pera, M. F., and Ying, Q. L. (2008) Germline Competent Embryonic Stem Cells Derived from Rat Blastocysts. *Cell* **135**, 1299-1310
23. Hickey, R. D., Mao, S. A., Glorioso, J., Lillegard, J. B., Fisher, J. E., Amiot, B., Rinaldo, P., Harding, C. O., Marler, R., Finegold, M. J., Grompe, M., and Nyberg, S. L. (2014) Fumarylacetoacetate hydrolase deficient pigs are a novel large animal model of metabolic liver disease. *Stem Cell Res* **13**, 144-153
24. Hickey, R. D., Mao, S. A., Glorioso, J., Elgilani, F., Amiot, B., Chen, H., Rinaldo, P., Marler, R., Jiang, H., DeGrado, T. R., Suksanpaisan, L., O'Connor, M. K., Freeman, B. L., Ibrahim, S. H., Peng, K. W., Harding, C. O., Ho, C. S., Grompe, M., Ikeda, Y., Lillegard, J. B., Russell, S. J., and Nyberg, S. L. (2016) Curative ex vivo liver-directed gene therapy in a pig model of hereditary tyrosinemia type 1. *Sci Transl Med* **8**, 349-399
25. Zhang, L., Shao, Y., Li, L., Tian, F., Cen, J., Chen, X., Hu, D., Zhou, Y., Xie, W., Zheng, Y., Ji, Y., Liu, M., Li, D., and Hui, L. (2016) Efficient liver repopulation of transplanted hepatocyte prevents cirrhosis in a rat model of hereditary tyrosinemia type I. *Sci Rep* **6**, 31460
26. Kuijk, E. W., Rasmussen, S., Blokzijl, F., Huch, M., Gehart, H., Toonen, P., Begthel, H., Clevers, H., Geurts, A. M., and Cuppen, E. (2016) Generation and characterization of rat liver stem cell

lines and their engraftment in a rat model of liver failure. *Sci Rep* **6**, 22154
27. Wang, Y., Fan, N., Song, J., Zhong, J., Guo, X., Tian, W., Zhang, Q., Cui, F., Li, L., Newsome, P. N., Frampton, J., Esteban, M. A., and Lai, L. (2014) Generation of knockout rabbits using transcription activator-like effector nucleases. *Cell Regen* **3**, 3
28. Bosze, Z., and Houdebine, L. M. (2006) Application of rabbits in biomedical research: A review. *World Rabbit Sci* **14**, 1-14
29. Goodman, Z. D. (2007) Grading and staging systems for inflammation and fibrosis in chronic liver diseases. *J Hepatol* **47**, 598-607
30. Elgilani, F., Mao, S. A., Glorioso, J. M., Yin, M., Iankov, I. D., Singh, A., Amiot, B., Rinaldo, P., Marler, R. J., Ehman, R. L., Grompe, M., Lillegard, J. B., Hickey, R. D., and Nyberg, S. L. (2017) Chronic Phenotype Characterization of a Large-Animal Model of Hereditary Tyrosinemia Type 1. *Am J Pathol* **187**, 33-41
31. Schauwvlieghe, P. P., Jaeken, J., Kestelyn, P., and Claerhout, I. (2013) Confocal microscopy of corneal crystals in a patient with hereditary tyrosinemia type I, treated with NTBC. *Cornea* **32**, 91-94
32. Gissen, P., Preece, M. A., Willshaw, H. A., and McKiernan, P. J. (2003) Ophthalmic follow-up of patients with tyrosinaemia type I on NTBC. *J Inherit Metab Dis* **26**, 13-16
33. Trautwein, C., Rakemann, T., Malek, N. P., Plumpe, J., Tiegs, G., and Manns, M. P. (1998) Concanavalin A-induced liver injury triggers hepatocyte proliferation. *J Clin Invest* **101**, 1960-1969
34. Ferrari, A., Hannouche, D., Oudina, K., Bourguignon, M., Meunier, A., Sedel, L., and Petite, H. (2001) In vivo tracking of bone marrow fibroblasts with fluorescent carbocyanine dye. *J Biomed Mater Res* **56**, 361-367
35. Li, Y., Song, Y., Zhao, L., Gaidosh, G., Laties, A. M., and Wen, R. (2008) Direct labeling and visualization of blood vessels with lipophilic carbocyanine dye DiI. *Nat Protoc* **3**, 1703-1708
36. Seok, J., Warren, H. S., Cuenca, A. G., Mindrinos, M. N., Baker, H. V., Xu, W., Richards, D. R., McDonald-Smith, G. P., Gao, H., Hennessy, L., Finnerty, C. C., Lopez, C. M., Honari, S., Moore, E. E., Minei, J. P., Cuschieri, J., Bankey, P. E., Johnson, J. L., Sperry, J., Nathens, A. B., Billiar, T. R., West, M. A., Jeschke, M. G., Klein, M. B., Gamelli, R. L., Gibran, N. S., Brownstein, B. H., Miller-Graziano, C., Calvano, S. E., Mason, P. H., Cobb, J. P., Rahme, L. G., Lowry, S. F., Maier, R. V., Moldawer, L. L., Herndon, D. N., Davis, R. W., Xiao, W., Tompkins, R. G., Inflammation, and Host Response to Injury, L. S. C. R. P. (2013) Genomic responses in mouse models poorly mimic human inflammatory diseases. *Proc Natl Acad Sci U S A* **110**, 3507-3512
37. Brem, G., Brenig, B., Goodman, H. M., Selden, R. C., Graf, F., Kruff, B., Springman, K., Hondele, J., Meyer, J., Winnacker, E. L., and Krausslich, H. (1985) Production of Transgenic Mice, Rabbits and Pigs by Microinjection into Pronuclei. *Reprod Domest Anim* **20**, 251-252
38. Hammer, R. E., Pursel, V. G., Rexroad, C. E., Wall, R. J., Bolt, D. J., Ebert, K. M., Palmiter, R. D., and Brinster, R. L. (1985) Production of Transgenic Rabbits, Sheep and Pigs by Microinjection. *Nature* **315**, 680-683
39. Tian, J., Song, J., Li, H., Yang, D., Li, X., Ouyang, H., and Lai, L. (2012) Effect of donor cell type on nuclear remodelling in rabbit somatic cell nuclear transfer embryos. *Reprod Domest Anim*

47, 544-552

40. Yuan, L., Sui, T., Chen, M., Deng, J., Huang, Y., Zeng, J., Lv, Q., Song, Y., Li, Z., and Lai, L. (2016) CRISPR/Cas9-mediated GJA8 knockout in rabbits recapitulates human congenital cataracts. *Sci Rep* **6**, 22024
41. Flisikowska, T., Thorey, I. S., Offner, S., Ros, F., Lifke, V., Zeitler, B., Rottmann, O., Vincent, A., Zhang, L., Jenkins, S., Niersbach, H., Kind, A. J., Gregory, P. D., Schnieke, A. E., and Platzer, J. (2011) Efficient immunoglobulin gene disruption and targeted replacement in rabbit using zinc finger nucleases. *PLoS One* **6**, e21045
42. Ji, D., Zhao, G., Songstad, A., Cui, X., and Weinstein, E. J. (2015) Efficient creation of an APOE knockout rabbit. *Transgenic Res* **24**, 227-235
43. Yan, Q., Zhang, Q., Yang, H., Zou, Q., Tang, C., Fan, N., and Lai, L. (2014) Generation of multi-gene knockout rabbits using the Cas9/gRNA system. *Cell Regen (Lond)* **3**, 12
44. Fu, Y., Foden, J. A., Khayter, C., Maeder, M. L., Reyon, D., Joung, J. K., and Sander, J. D. (2013) High-frequency off-target mutagenesis induced by CRISPR-Cas nucleases in human cells. *Nat Biotechnol* **31**, 822-826
45. Yang, D., Song, J., Zhang, J., Xu, J., Zhu, T., Wang, Z., Lai, L., and Chen, Y. E. (2016) Identification and characterization of rabbit ROSA26 for gene knock-in and stable reporter gene expression. *Sci Rep* **6**, 25161
46. Macsai, M. S., Schwartz, T. L., Hinkle, D., Hummel, M. B., Mulhern, M. G., and Rootman, D. (2001) Tyrosinemia type II: nine cases of ocular signs and symptoms. *Am J Ophthalmol* **132**, 522-527
47. Reese, J. A., and Byard, J. L. (1981) Isolation and culture of adult hepatocytes from liver biopsies. *In vitro* **17**, 935-940

FOOTNOTES

This work was supported by grants from The National Key Research and Development Program of China (2016YFA0100102), the National Natural Science Foundation of China (NSFC; 31401275), Guangdong Province Science and Technology program (2013B050800010, 2013B060300017, 2014030304010, 2014B030301058, 2014A030312001, 2015B020229002, and 2016B030229007), Guangzhou Science and Technology Cooperation program (2012J5100040 and 201508030027), the Key Deployment Project of the Chinese Academy of Sciences (KSZD-EW-Z-005-003-002), and the NSFC and Hong Kong Research Grants Council (RGC) joint research fund (81261160506). The abbreviations used are: ALT, alanine aminotransferase; AST, aspartate aminotransferase; CRISPR, clustered regularly interspaced short palindromic repeats; Cas9, CRISPR-associated protein 9; ESCs, embryonic stem cells; F0, founder generation; F1, first filial generation; FAH, fumarylacetoacetate hydroxylase; HT1, hereditary tyrosinemia type 1; NTBC, 2-(2-nitro-4-trifluoromethylbenzoyl)-1,3-cyclohexanedion; TALENs, transcription activator-like effector nucleases.

Table I: Generation of *Fah* knockout rabbits using TALENs.

No. surrogates	TALEN mRNA concentration (ng/μL)	No. embryos transferred	No. newborns (%)	No. mutant rabbits (%)
3	10	34	6 (12)	0
3	20	39	12 (31)	3 (25)
2	30	32	9 (28)	5 (56)
3	50	37	4 (11)	4 (100)
4	100	40	0	0

FIGURE LEGENDS

Figure 1: **Preparation of TALENs and generation of *Fah* knockout rabbits. A**) Design of TALENs targeting exon 2 of rabbit *Fah* gene. Bases in red indicate the TALEN recognition sequences. **B**) Sanger sequencing of the targeted region in the *Fah* locus in F0 rabbits; * represents rabbits in which wild-type *Fah* sequence was detected. **C**) Sanger sequencing of the targeted region in the *Fah* locus in $Fah^{-/-}$ F1 rabbits. **D**) Schematic of the 3 groups of $Fah^{-/-}$ rabbits used to study the dependence on NTBC for long-term survival (ON: NTBC is administered; OFF: NTBC withdrawal). **E**) Survival curve for the same 3 groups of $Fah^{-/-}$ rabbits. **F**) Western blotting analysis confirms that $Fah^{-/-}$ rabbits (-/-) are negative for FAH protein expression in liver tissue lysates, whilst $Fah^{+/-}$ (+/-) rabbits express reduced amount of FAH. Band intensities (FAH/ACTIN) were quantified using ImageJ software and shown as relative to wild-type (+/+) rabbits.

Figure 2: $Fah^{-/-}$ rabbits develop progressive liver failure in the absence of NTBC. A) Severe necrosis in the liver of a $Fah^{-/-}$ rabbit (right) belonging to group 3 of NTBC administration (as in Figure 1D), in contrast to a healthy wild-type rabbit. **B**) Immunohistochemistry (IHC) of liver and kidney sections of a $Fah^{-/-}$ rabbit belonging to group 2 of NTBC administration show no expression of FAH, in contrast to a wild-type rabbit. Scale bars: 50 μm. **C**) Hematoxylin and eosin (HE) staining shows abnormal tissue architecture in liver and kidney sections of the same $Fah^{-/-}$ rabbit in B, in contrast to a wild-type rabbit. In the $Fah^{-/-}$ rabbit, diffused hepatocellular injury with dysplastic hepatocytes and tubular epithelial injury of kidney were observed. Scale bars: 50 μm. **D**) Picrosirius red staining shows the existence of mild interstitial fibrosis in the liver of the same $Fah^{-/-}$ rabbit in A but not in the wild-type rabbit. Scale bars: 50 μm. **E**) Serum biochemical parameters indicate liver damage in $Fah^{-/-}$ rabbits compared to a wild-type rabbit. TG stands for triglycerides. Data were presented as mean ± standard error of the mean (SEM; n = 3 replicate measurements). * corresponds to $P < 0.01$ according to Student's *t*-test.

Figure 3: Ocular manifestations in *Fah* knockout rabbits. A) Photographs of right (OD) and left (OS) eyes of 2 $Fah^{+/-}$ rabbits show corneal abnormalities; a wild-type (WT) rabbit was used as control. **B**) Slit lamp photographs of the same 3 rabbits show abnormalities of chamber depth and lens opacification in $Fah^{+/-}$ rabbit number 1 compared to the wild-type. **C**) Measurement of intraocular pressure using ICAR tomometer (Icane, Finland) in the same 3 rabbits. Only the left eye of $Fah^{+/-}$ rabbit number 1 shows pathogenic levels. **D**) Hematoxylin and eosin staining shows corneal structural abnormalities (edema, thickening, cellular defects, and disorganization of the corneal epithelium and stroma) in the left eye of $Fah^{+/-}$ rabbit number 2 compared to the wild-type. Scale bars: 50 μm.

Figure 4: Hepatocyte transplantation of $Fah^{-/-}$ rabbits. A) Transplantation of wild-type rabbit primary hepatocytes into the liver of a wild-type rabbit treated with Concavalin A (ConA; 5.0 mg/kg, intrasplenic injection) to induce acute liver damage. Engraftment of DiI-labeled hepatocytes can be observed under the fluorescence microscope at 3 weeks post-transplantation. DAPI was used to stain nuclei. Scale bars: 50 μm. **B**) Schematic showing the allogeneic transplantation procedure in $Fah^{-/-}$ rabbits. NTBC was administered for another 2 days after the first liver biopsy. **C**) Engraftment of DiI-labeled cells observed under the fluorescence microscope in a $Fah^{-/-}$ rabbit without NTBC at 1 month post-transplantation. Scale

bars: 50 μm.

Figure 5: Wild-type primary hepatocyte transplantation rescues liver architecture and prevents death of *Fah*$^{-/-}$ rabbits. **A**) Top panels: FAH immunohistochemistry shows wild-type hepatocyte repopulation of the liver of a *Fah*$^{-/-}$ rabbit 1 month post-transplantation compared to the control (non-transplanted *Fah*$^{-/-}$ rabbit). Lower panels: hematoxylin and eosin staining shows restoration of liver architecture in the same transplanted *Fah*$^{-/-}$ rabbit compared to the non-transplanted *Fah*$^{-/-}$ rabbit. Scale bars: 50 μm. **B**) Body weight changes of the 2 *Fah*$^{-/-}$ rabbits in A (with or without transplantation) and a control wild-type rabbit. * corresponds to $P < 0.01$. **C**) Photographs of a transplanted *Fah*$^{-/-}$ rabbit at 3 months post-transplantation and a non-transplanted *Fah*$^{-/-}$ rabbit. The non-transplanted *Fah*$^{-/-}$ rabbit appears weak. **D and E**) Serum levels of ALT and AST in a wild-type and 2 *Fah*$^{-/-}$ rabbits (with or without transplantation). Data are presented as the means ± SEM (n = 3 replicate measurements). * corresponds to $P < 0.01$. **F**) FAH immunohistochemistry shows extensive wild-type hepatocyte repopulation of the liver of a *Fah*$^{-/-}$ rabbit 3 months post-transplantation compared to the non-transplanted *Fah*$^{-/-}$ rabbit. Scale bars: 50 μm. **G**) Right panel: hematoxylin and eosin staining shows restoration of liver architecture (circled by dashed lines) in the same transplanted *Fah*$^{-/-}$ rabbit at 3 months post-transplantation. Left panel: adjacent liver section of the transplanted *Fah*$^{-/-}$ rabbit showing co-localization of areas with normal structure and positive FAH staining. Scale bars: 50 μm.

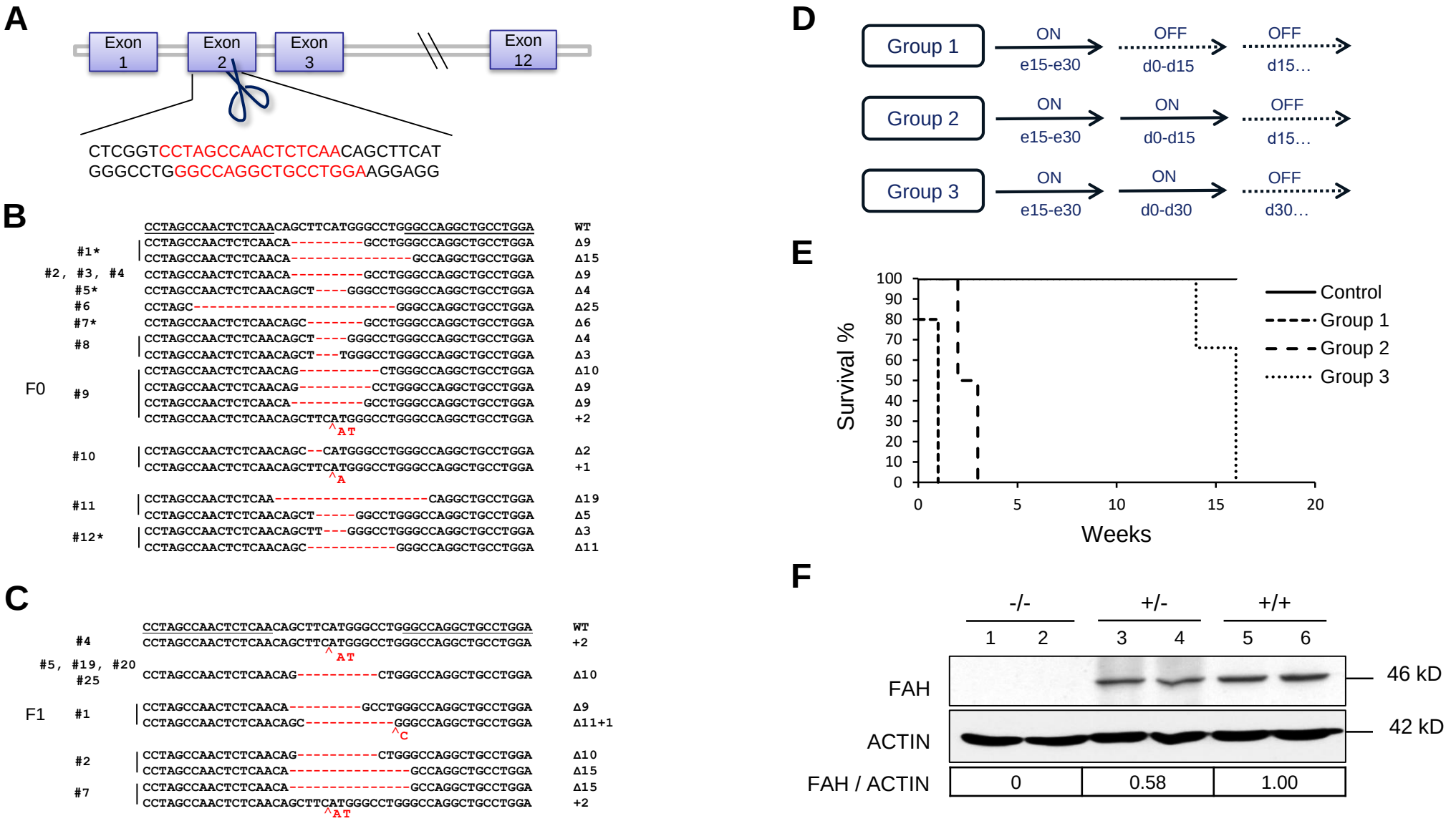

Figure 1

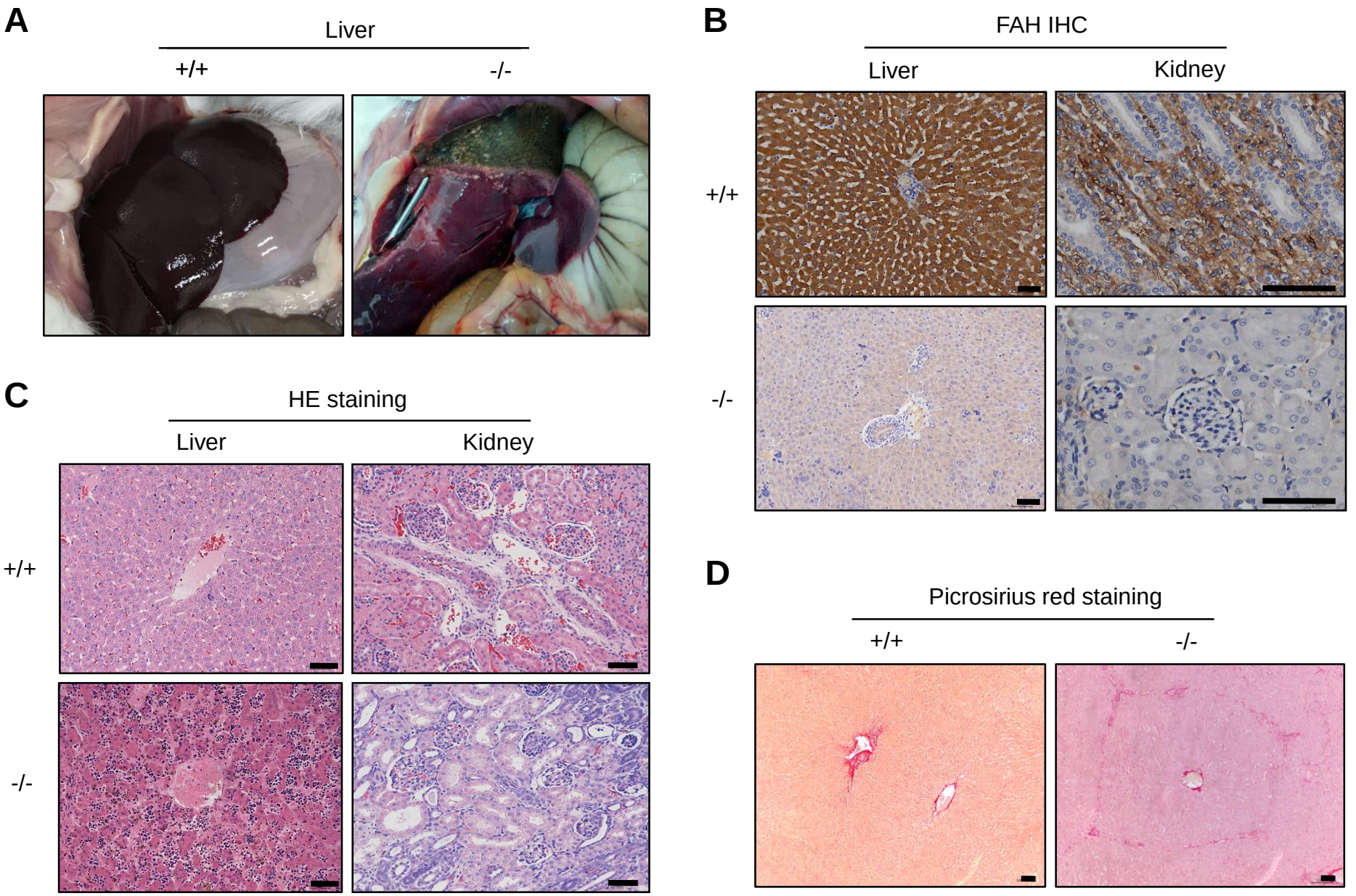

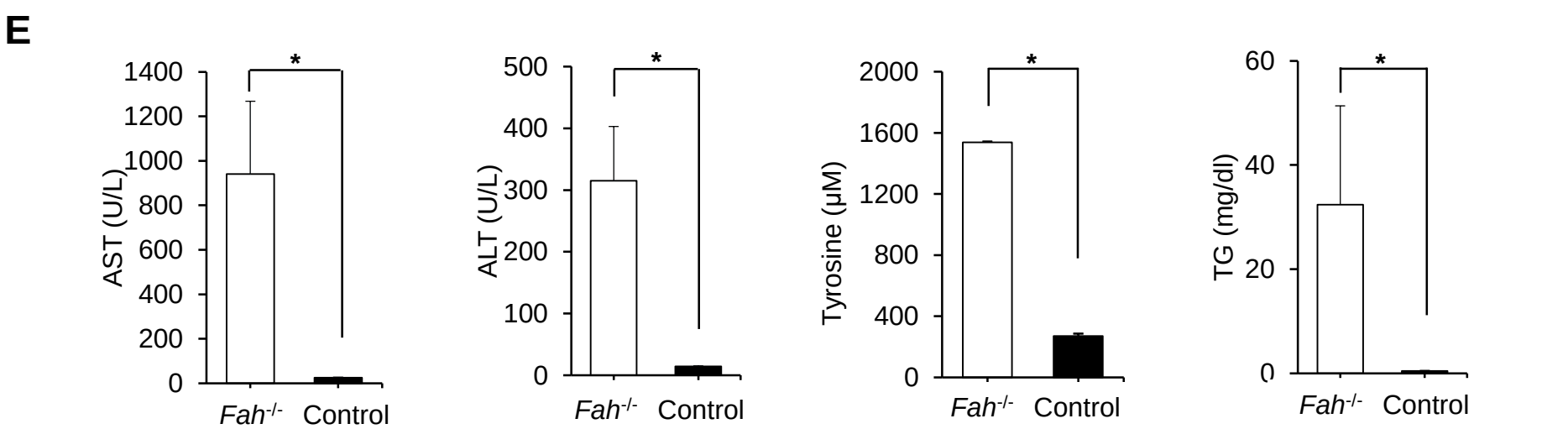

Figure 2

A

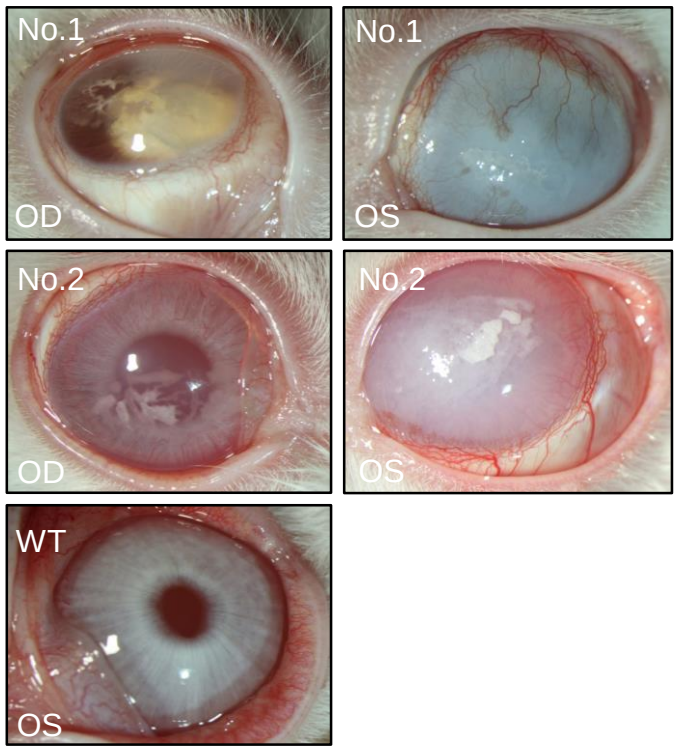

B

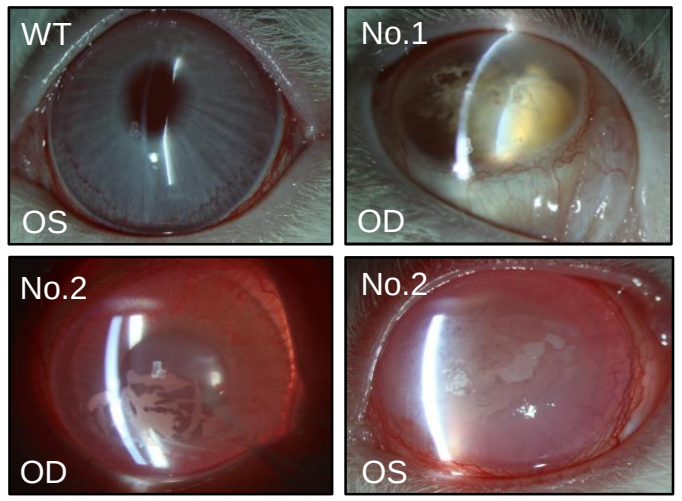

C

Eye pressure (mm Hg)			
	WT	No.1	No.2
OD	15.2	12	12.67
OS	12.14	48.33	10.33

D

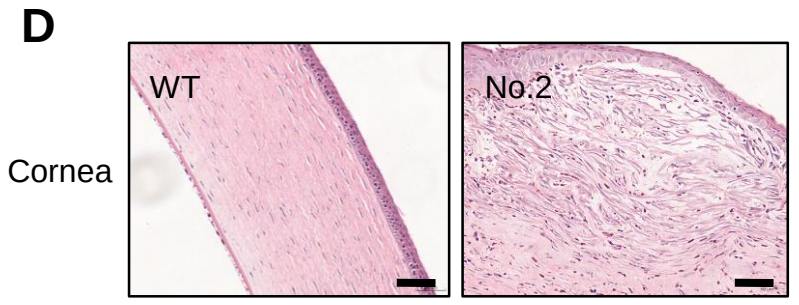

Figure 3

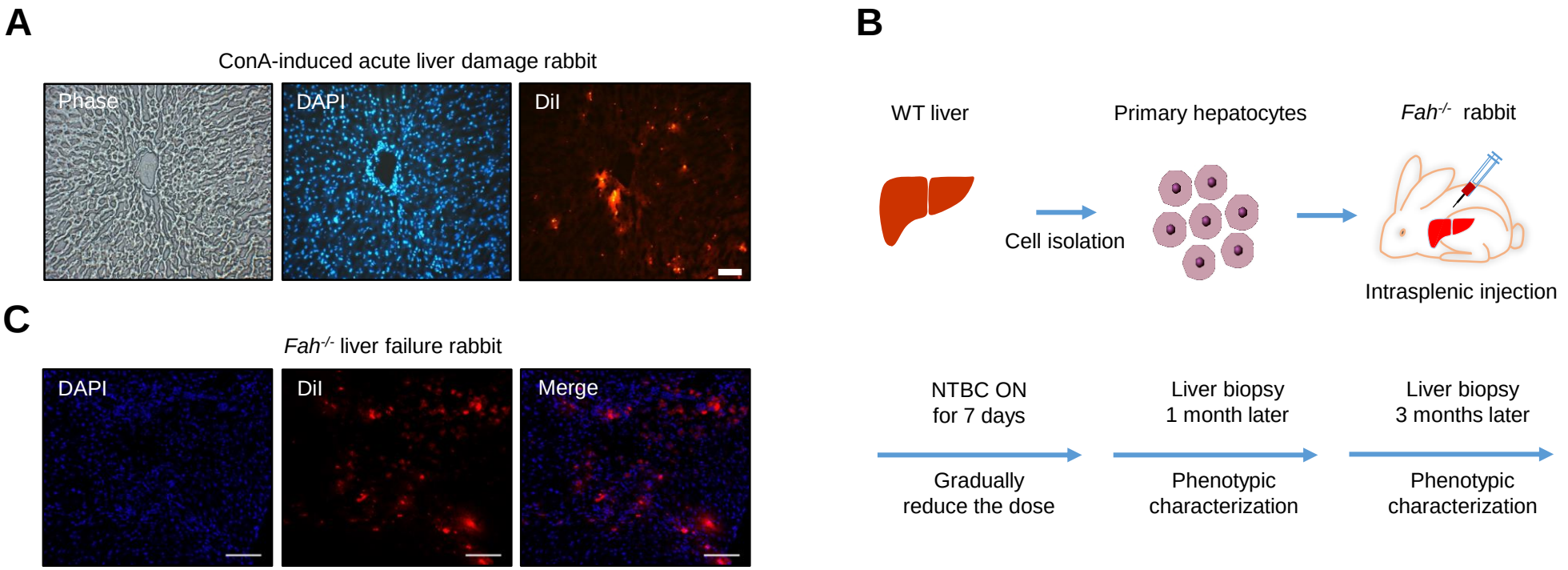

Figure 4

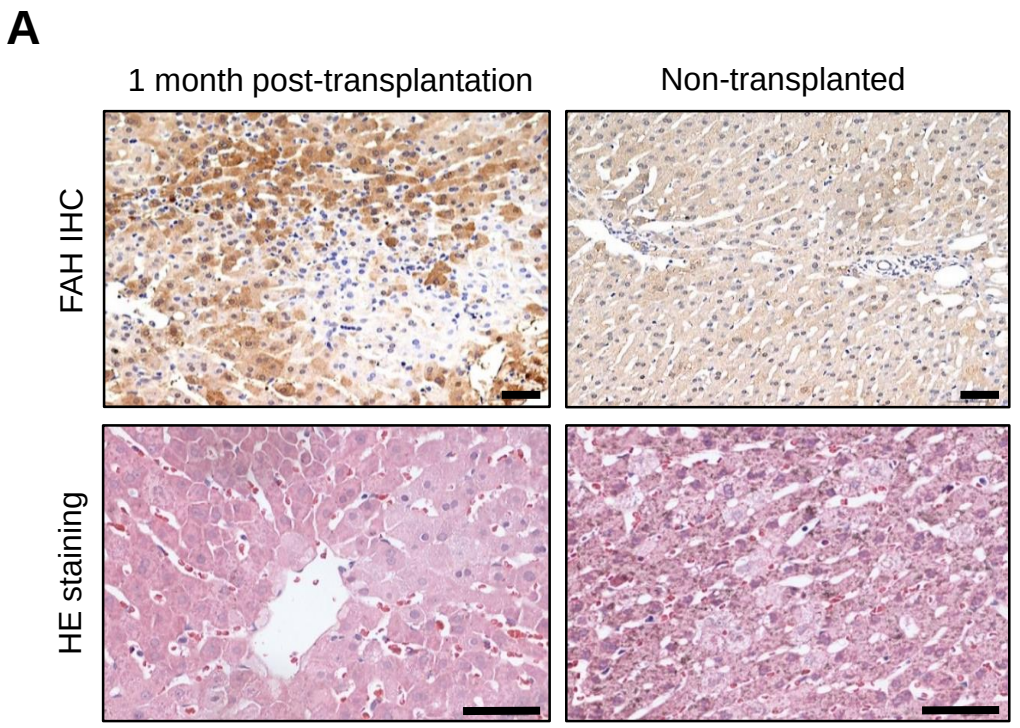

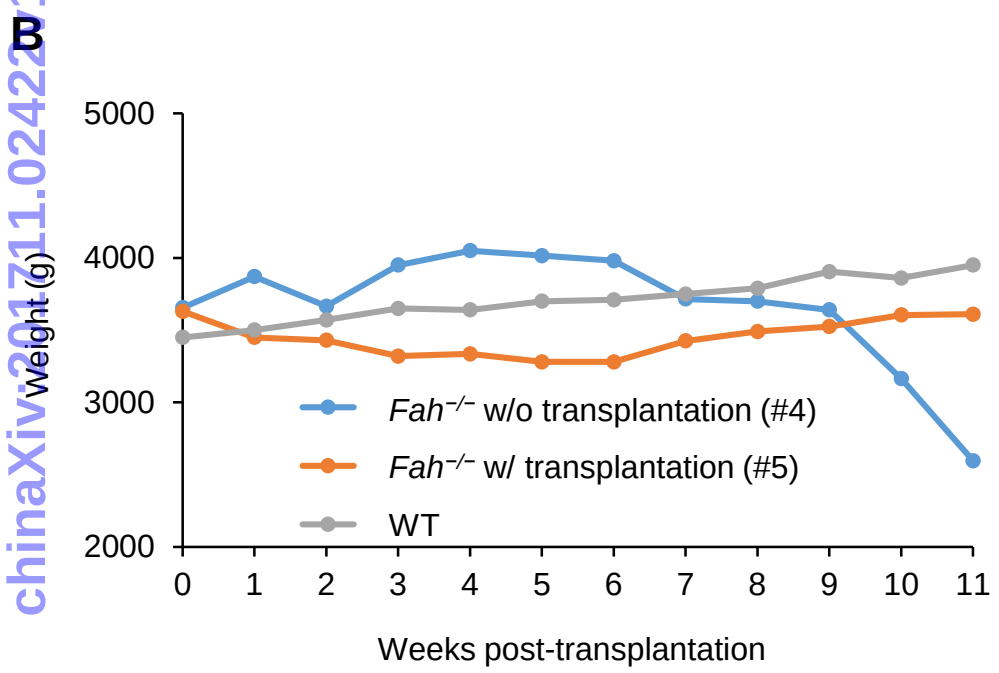

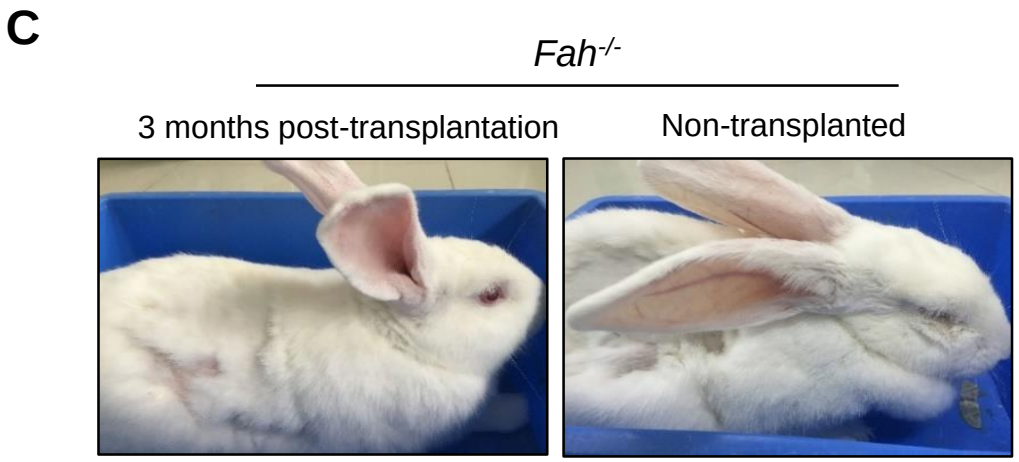

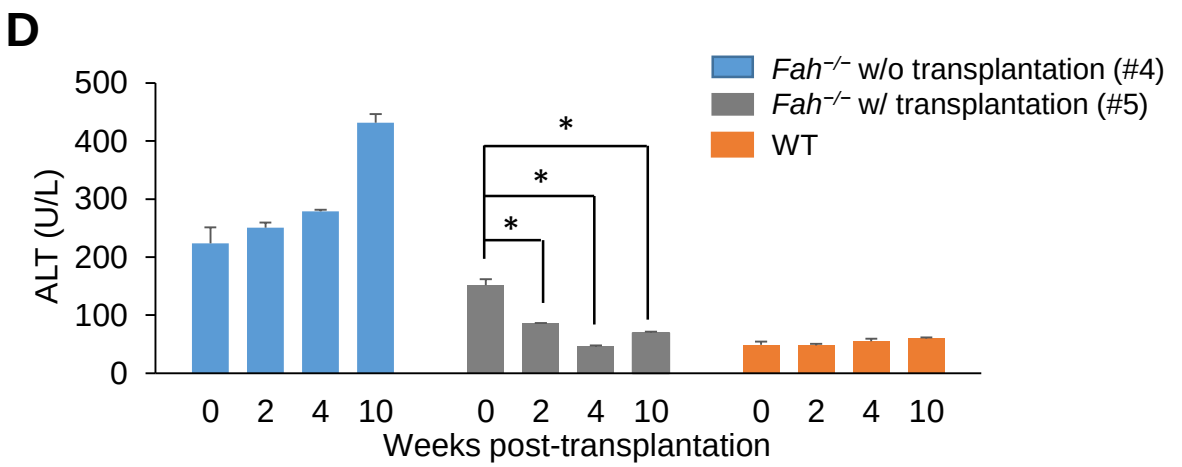

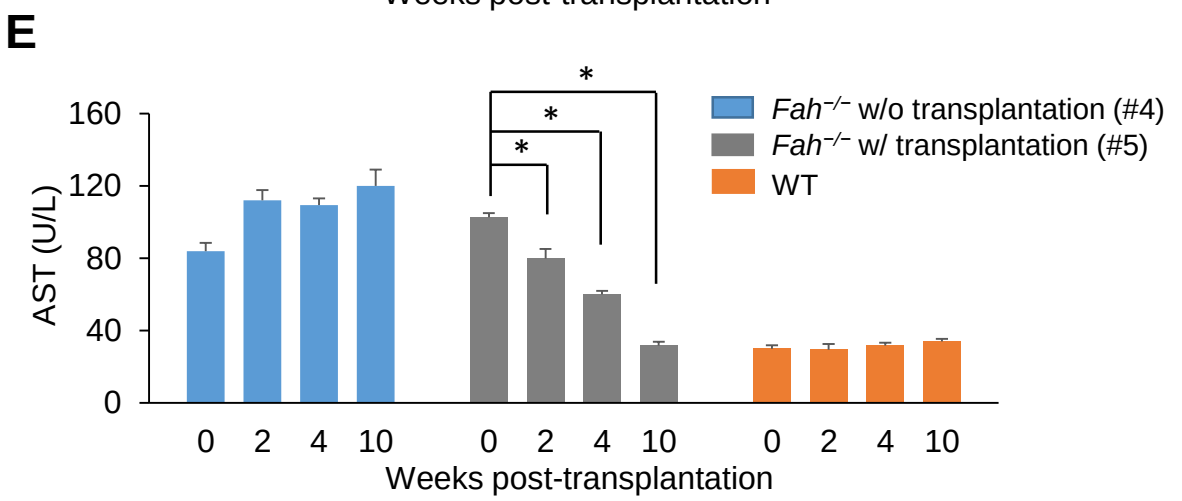

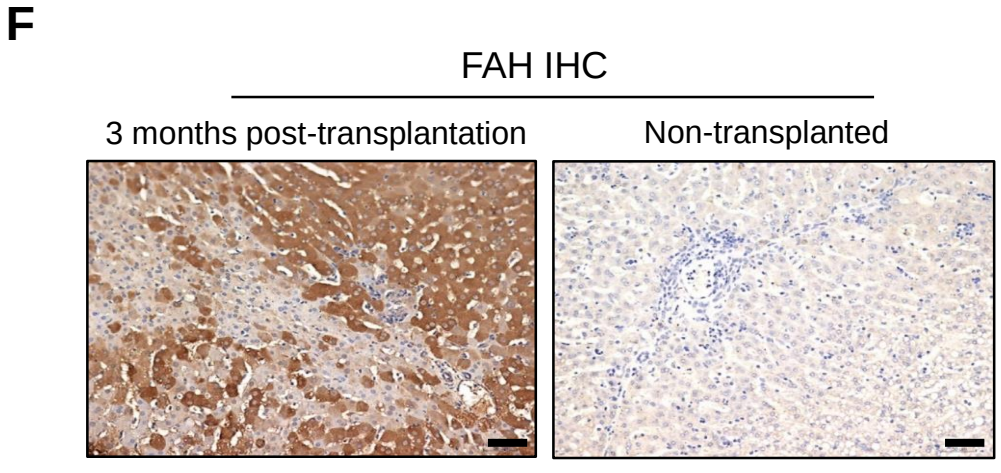

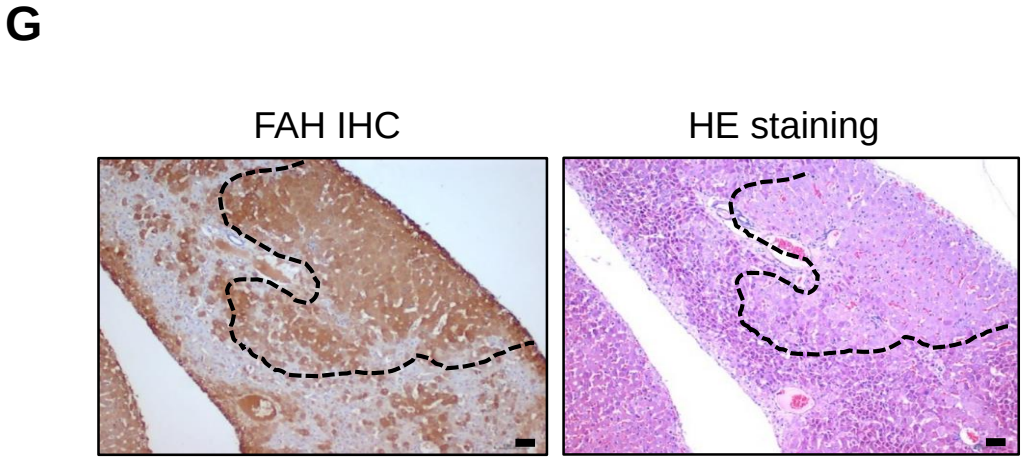

Figure 5